Research Paper

Procyanidin B2 mitigates endothelial endoplasmic reticulum stress through a PPARδ-Dependent mechanism

Xin Nie [a,1], Weiqi Tang [a,b,1], Zihui Zhang [b], Chunmiao Yang [b], Lei Qian [a], Xinya Xie [b], Erjiao Qiang [a], Jingyang Zhao [a,b], Wenfei Zhao [b], Lei Xiao [b,**], Nanping Wang [a,*]

[a] Advanced Institute for Medical Sciences, Dalian Medical University, Dalian, 116044, China
[b] Cardiovascular Research Center, School of Basic Medical Sciences, Xi'an Jiaotong University, Xi'an, 710061, China

ABSTRACT

Hyperglycemia-induced endothelial endoplasmic reticulum (ER) stress is implicated in the pathophysiology of diabetes and its vascular complications. Procyanidins are enriched in many plant foods and have been demonstrated to exert several beneficial effects on diabetes, cardiovascular and other metabolic diseases. In the present study, we investigated the effect of procyanidin B2 (PCB2), the most widely distributed natural procyanidin, on ER stress evoked by high glucose in endothelial cells (ECs) and the underlying mechanisms. We showed that PCB2 mitigated the high glucose-activated ER stress pathways (PERK, IRE1α and ATF6) in human vascular ECs. In addition, we found that PCB2 attenuated endothelial ER stress via the activation of peroxisome proliferator-activated receptor δ (PPARδ). We demonstrated that PCB2 directly bound to and activated PPARδ. Conversely, GSK0660, a selective PPARδ antagonist, attenuated the suppressive effect of PCB2 on the ER stress signal pathway. Functionally, PCB2 ameliorated the high glucose-impaired endothelium-dependent relaxation in mouse aortas. The protective effect of PCB2 on vasodilation was abolished in the aortas pretreated with GSK0660 or those from the EC-specific PPARδ knockout mice. Moreover, the protective effects of PCB2 on ER stress and endothelial dysfunction required the inter-dependent actions of PPARδ and AMPK. Collectively, we demonstrated that PCB2 mitigated ER stress and ameliorated vasodilation via a PPARδ-mediated mechanism beyond its classic action as a scavenger of free radicals. These findings further highlighted the novel roles of procyanidins in intervening the ER stress and metabolic disorders related to endothelial dysfunction.

1. Introduction

Endoplasmic reticulum (ER) is an important eukaryotic organelle responsible for protein translation, modifications and folding. Increased demands or pathophysiological perturbations result in accumulation and aggregation of unfolded or misfolded proteins within ER, a state known as "ER stress" [1]. An intrinsic machinery has evolved to sense the ER stress and initiate the unfolded protein response (UPR). The UPR pathways involve three ER transmembrane proteins: protein kinase RNA-like endoplasmic reticulum kinase (PERK), inositol requiring enzyme 1 (IRE1) and activating transcription factor 6 (ATF6) [2]. Under ER stress causes the dissociation of an ER chaperon protein the 78 kDa glucose-regulated protein (GRP78) from and activates the UPR pathways, leading to downstream transcriptional activation of UPR target genes to regulate the protein synthesis, degradation, oxidative stress, inflammation and apoptosis [3]. Aberrant ER stress is implicated in the

pathogeneses of various metabolic and pro-inflammatory diseases including diabetes and cardiovascular diseases [4]. The markers for ER stress were observed at athero-prone areas in the arteries from diabetic obese mice [5]. On the other hand, many diabetogenic and atherogenic risk factors such as high levels of glucose [6], free fatty acid [7] and modified LDL [8] are known to instigate ER stress which, in turn, results in endothelial dysfunction [9].

Epidemiological studies suggested that fruit and vegetable consumptions are significantly correlated with the reduced risks of metabolic disorders such as type 2 diabetes, obesity and cardiovascular diseases [10]. These beneficial effects are thought to be partly attributed to the anti-oxidative and free radical scavenging properties of the polyphenols that are enriched in such diets [11]. Procyanidins, a subclass of polyphenolic compounds, are widely distributed in plants including fruits, vegetables, nuts, beans, and tea and are integral part of the human diet [12]. Their anti-oxidative ability makes them potentially important compounds in the prevention or treatment of metabolic disorders although the in vivo metabolism, distribution and bio-availabilities could be limiting factors [13]. B-type procyanidin (PCB2) is the most ubiquitous proanthocyanidin enriched in apple, cherries, cocoa and grape seeds. It is a dimer formed between 2 flavan-3-ol (−)-epicatechins. PCB2 could be readily detected in human circulation after dietary consumption [14]. In addition, tissue distribution of PCB2 and its metabolites had also been recently profiled [15]. Therefore, we investigated whether PCB2 could mitigate ER stress in ECs and diabetes-related endothelial dysfunction and elucidated the underlying molecular mechanisms.

2. Methods

2.1. Reagents

PCB2, phenylephrine (Phe), acetylcholine (ACh), sodium nitroprusside (SNP), 1H-Oxadiazolo [[3,4],-a] quinoxalin-1-one (ODQ), indomethacin, compound C (CC), GW501516, mannitol, palmitate acid (PA), D-glucose, dihydroethidium (DHE), A23187 and tunicamycin (TM) were from Sigma-Aldrich (St. Louis, MO, USA). NG-nitro-L-arginine methyl ester (L-NAME), 1400W and GSK0660 were from Tocris Bioscience (Bristol, UK). L-012 was from Wako Pure Chemical Industries (Osaka, Japan). Recombinant human PPARδ protein and anti-phosphorylated IRE1α (Ser^{724}) antibody were obtained from Abcam (Cambridge, MA, USA). Antibodies against adenosine monophosphate-activated protein kinase (AMPK), phospho-AMPK (Thr^{172}), activating transcription factor 4 (ATF4), ATF6, GRP78, protein-disulfide isomerase (PDI), IRE1α and Griess reagent nitrite measurement kit were from Cell Signaling Technology (Danvers, MA, USA). Antibodies against PERK and phospho-PERK (Thr^{981}), 4-Amino-5--methylamino-2′,7′-difluorofluorescein diacetate (DAF-FM DA) were from ThermoFisher Scientific (Waltham, MA, USA). Antibody against β-actin and horseradish peroxidase (HRP)-conjugated secondary antibodies were from Santa Cruz Biotechnology (Santa Cruz, CA, USA).

2.2. Animals

Male C57BL/6J mice, endothelium-specific PPARδ knockout mice (PPARδ$^{flox/flox}$, Cre$^+$; PPARδ$^{EC-/-}$) and their wild-type littermates (PPARδ$^{flox/flox}$, Cre$^-$; WT) aged 8–10 weeks and weighing 20–25 g were used for this study. PPARδ$^{EC-/-}$ mice were generated by crossing the PPARδ$^{flox/flox}$ mice, which harbored the loxP sites flanking exon 4 of the murine Ppard gene, with the Tie2-Cre mice (Jackson Laboratory, Bar Harbor, ME, USA) as previously described [16]. The mice were housed in a temperature-controlled holding room (22–23 °C) with a 12-h light/dark cycle and fed standard chow and water. All animal care and experimental procedures were conducted in accordance with the National Institutes of Health Guide for the Care and Use of Laboratory Animals with the approval by the Animal Research Committee of Xi'an Jiaotong University (No. XJTULAC2017-729). Mice were euthanized

using CO_2 method following 2013 AVMA guidelines [17].

2.3. Cell culture

Human umbilical vein endothelial cells (HUVECs) were maintained in M199 containing 20% fetal bovine serum (FBS), streptomycin (100 U/ml), penicillin (0.1 mg/ml), fibroblast growth factor (FGF, 10 ng/ml), heparin (0.1 mg/ml) and L-glutamine (2 mM). HUVECs within 3 passages were used unless otherwise indicated. Bovine aortic endothelial cells (BAECs) were cultured in DMEM with 10% FBS and antibiotics.

2.4. Vascular reactivity

After mice were sacrificed, thoracic aortas were removed and cleaned of adhesive tissues in oxygenated ice-cold sterile Krebs solution. Aortic rings (2-mm in length) were incubated in DMEM supplemented with 10% FBS, plus 100 U/ml penicillin and 0.1 mg/ml streptomycin, in a CO_2 incubator with 95% O_2 plus 5% CO_2 [16]. The aortic rings were incubated with high glucose (HG, 30 mM) in the presence or absence of PCB2 (10 μM) and/or GSK0660 (1 μM), CC (20 μM). Mannitol was used as the osmolarity control for the HG treatment. The relaxation capacity of aortic rings to ACh was largely preserved after the ex vivo organ culture under the basal condition. After incubation, the aortic rings were transferred to fresh Krebs solution for functional studies in Myograph system (Danish Myo Technology, Aarhus, Denmark) to measure vaso-relaxation. The changes of isometric tension were recorded using PowerLab Data Acquisition System (Harvard Apparatus, Holliston, MA, USA). All rings were stretched to an optimal baseline tension (3 mN) and equilibrated for 1 h before the contraction by phenylephrine (Phe, 10 μM). We also detected the relaxation in response to SNP for endothelium-independent relaxation.

2.5. Surface plasmon resonance (SPR) analysis

SPR analysis was used to measure the binding interactions of PCB2 and PPARδ as previously described [18]. Briefly, recombinant PPARδ protein was immobilized on CM5 sensor chip (Biacore-GE Healthcare, Piscataway, NJ, USA) by amine coupling reaction with final response at 5000 response units. The surface was blocked with ethanolamine (pH 8.5, 1 M). A two-fold variable concentration dilution series of PCB2 were injected into the chip at a flow rate of 30 μl/min for 90 s and followed by dissociation (120 s). All binding analyses were performed in PBS with 0.05% tween-20 and 1% DMSO at 25 °C (pH 7.4). We calculated the equilibrium dissociation constant (Kd) based on 1:1 Langmuir binding model using Biacore evaluation software.

2.6. Luciferase reporter assay

The plasmids expressing PPARδ or vector control (pcDNA3.1) were co-transfected with the plasmid expressing the PPARδ-responsive element (PPRE)-TK-driven luciferase reporter (pPPRE-TK-luc) into BAECs with the use of Lipofectamine 2000 (Invitrogen, Carlsbad, CA, USA). Cell lysates were harvested to measure the luciferase activity by using the luciferase reporter assay system (Promega, Madison, WI, USA) [19]. The β-galactosidase plasmid (pRSV-gal) was also transfected to normalize the transfection efficiency.

2.7. Quantitative reverse-transcriptase-PCR (qRT-PCR)

Total RNA was isolated from HUVECs with Trizol Reagent (Life Technologies) and used for cDNA synthesis by using iScript cDNA synthesis kit (Bio-rad, Hercules, CA, USA). qRT-PCR was performed with the GoTaq qPCR Master Mix (Promega) and a 7500 qPCR System (Applied Biosystems, Foster City, CA, USA). The mRNA expressions wereexamined using specific primers: C/EBP homologous protein (CHOP), 5′-GGAAACAGAGTGGTCATTCCC-3' (forward)

and 5′-GGAAACAGAGTGGTCATTCCC-3' (reverse); GRP78, 5′- TCTGCTTGATGTGTGTCCTCTT-3' (forward) and 5′-GTCGTTCACCTTCGTAGACCT-3' (reverse); ATF4, 5′-CTCCGGGA CAGATTGGATGTT-3' (forward) and 5′-GGCTGCTTATTAGTCTCCTG-GAC-3' (reverse); ATF3, 5′- CTCTGCCTCGGAAGTGAGTG-3' (forward) and 5′-CTTCTTCAGGGGCTACCTCG-3' (reverse); adipose different iation-related protein (ADRP), 5′-TCAGCTCCATTCTACTGTTCACC-3' (forward) and 5′-TCAGCTCCATTCTACTGTTCACC-3' (reverse); pyruvate dehydrogenase kinase 4 (PDK4), 5′-AGGTC-GAGCTGTTCTCCCGCT-3' (forward) and 5′-GCGGTCAGGCAG GATGTCAAT-3' (reverse); angiopoietin-like 4 (ANGPTL4), 5′-AAA-GAGGCTGCCCGAGAT-3' (forward) and 5′- GCGCCTCTGAAT-TACTGTCC-3' (reverse); glyceraldehyde-3-phosphate dehydrogenase (GAPDH), 5′-ACCACAGTCCATGCCATCAC-3' (forward) and 5′-TCCAC-CACCCTGTTGCTGTA-3' (reverse). Fold changes of gene expression were calculated using the $2^{-\Delta\Delta Ct}$ method. GAPDH was used as an internal control.

2.8. Western blotting

Cellular proteins were extracted with lysis buffer (50 mM Tris-HCl, pH 7.5, 15 mM EGTA, 100 mM NaCl, 0.1% Triton X-100 and complete protease and phosphatase inhibitor cocktail). Protein extracts were resolved on 10% SDS-PAGE. PVDF blots were reacted with specific antibodies and HRP-labeled secondary antibodies, followed by enhanced chemiluminescence (ECL) detection. The intensities of the bands were quantified by using Image J software from NIH Image.

2.9. Measurement of NO production

Intracellular NO production was detected using a NO-sensitive fluorescent dye DAF-FM DA as previously described [16]. The cells were washed with ice-cold PBS and incubated with 5 μM DAF-FM DA for 30 min in the dark at 37 °C. NO production in response to A23187 (1 μM, calcium ionophore) was evaluated by measuring the fluorescence intensity with a confocal microscope (Ex/Em: ~495/515 nm). Results were presented as a ratio of the fluorescence intensities before and after the addition of A23187 (F1/F0).

Release of NO was also indirectly assessed by measuring the concentration of nitrite (NO_2^-), a stable oxidization product of NO, in the supernatants of HUVECs. Using a Griess Reagent System kit according to the manufacturer's instructions, the nitrite concentration was determined spectrophotometrically at 550 nm [20]. The results were expressed as μM nitrite/10^5 cells.

2.10. Measurement of reactive oxygen species (ROS)

Intracellular ROS level was determined by using the luminol derivative L-012 [8-amino-5-chloro-7-phenylpyridol [[3,4],-d] pyridazine-1, 4 (2H, 3H) dione] [16]. ECs were plated and incubated with L-012 (100 μM) at 37 °C in dark for 30 min. The chemiluminescence was measured on a VICTOR TM X2 luminescence microplate reader (PerkinElmer, Seattle, WA, USA). ROS was also measured by using DHE (a superoxide-sensitive dye) staining. ECs were incubated with DHE (5 μM, 30 min, 37 °C). DHE fluorescence was examined under fluorescence microscopy (Ex/Em: ~510/580 nm).

2.11. Preparation of palmitic acid

BSA-conjugated palmitic acid (PA, 16:0) was prepared as described previously [16]. Briefly, PA was dissolved in 50% ethanol at 65 °C for 15 min to obtain a stock solution, concentration of 150 mM. Aliquots of stock solution were emulsified with fatty acid-free BSA (Sigma) by incubation for 1 h at 37 °C. The final molar ratio of PA/BSA was 5:1. The control condition included a solution of vehicle (ethanol/water, 1:1, vol/vol) mixed with BSA at the same concentration as the PA solution.
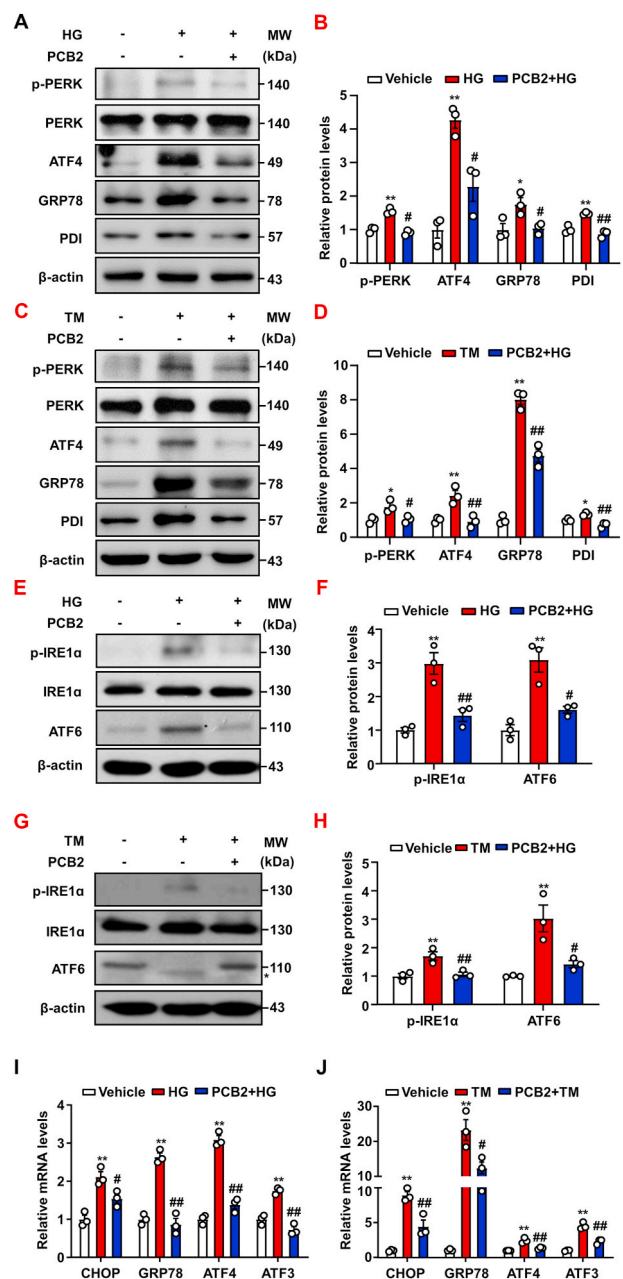
Fig. 1. PCB2 attenuated high glucose-triggered ER stress in ECs. HUVECs were pretreated with or without PCB2 (10 μM, 12 h) before the exposure to high glucose (HG, 30 mM) or mannitol for 24 h. **(A)** Protein levels of p-PERK, PERK, ATF4, GRP78 and PDI were detected by using western blotting. **(B)** Quantification of p-PERK/PERK, ATF4, GRP78 and PDI levels as in (A) (n = 3). **(C)** HUVECs were pretreated with or without PCB2 (10 μM, 12 h) before the exposure to tunicamycin (TM, 2 μg/ml) for 16 h. Protein levels of p-PERK, PERK, ATF4, GRP78 and PDI were detected. **(D)** Quantification of p-PERK/ PERK, ATF4, GRP78 and PDI levels as in (C) (n = 3). **(E, G)** Protein levels of p-IRE1α, IRE1α and ATF6 were assessed, *, deglycosylated ATF6. **(F, H)** Quantification of p-IRE1α/IRE1α and ATF6 levels as in (E) and (G) (n = 3). **(I, J)** The mRNA levels of CHOP, GRP78, ATF4 and ATF3 were assessed by using qRT-PCR (n = 3). All data were expressed as mean ± SEM. *$P < 0.05$, **$P < 0.01$ vs. Vehicle; #$P < 0.05$, ##$P < 0.01$ vs. HG or TM.

2.12. Statistical analysis

Results were expressed as mean ± SEM. The statistical differences between two groups were analyzed using Student *t*-test. One-way ANOVA with post hoc tests was performed for those among multiple
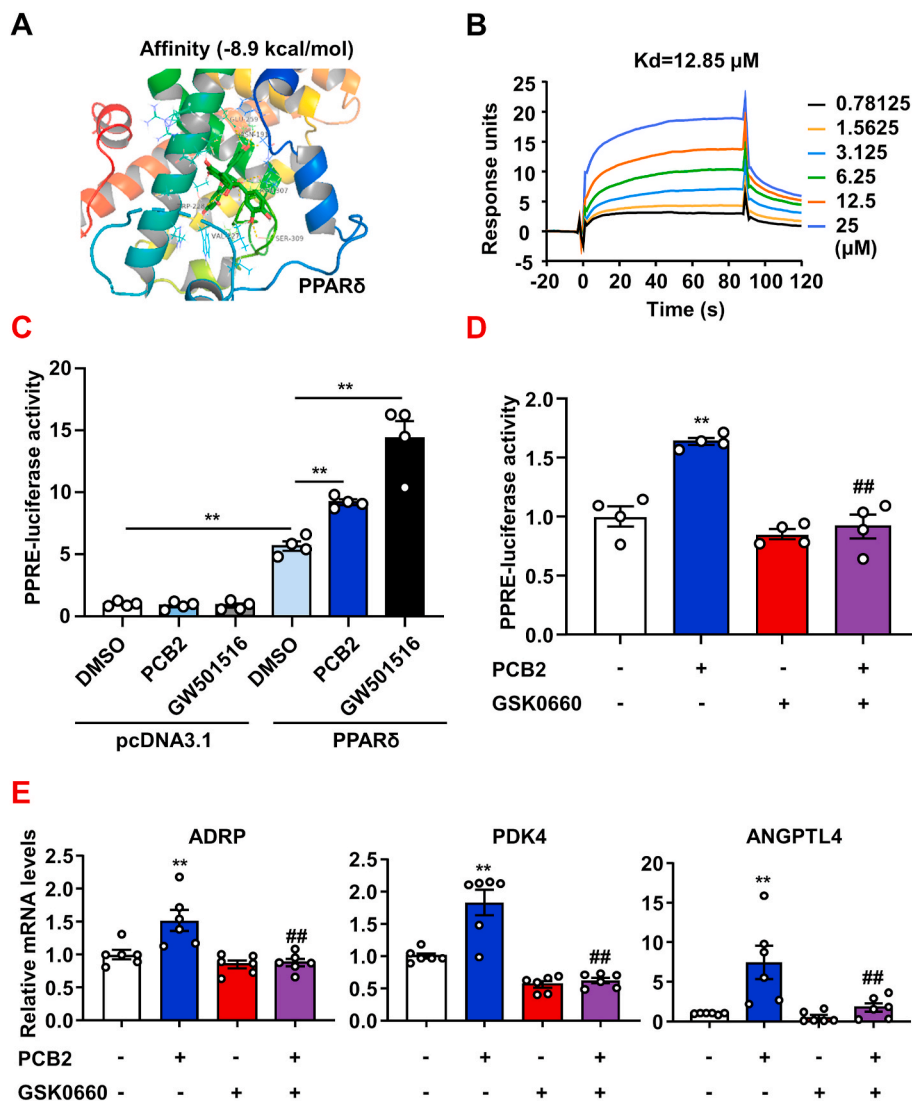
Fig. 2. PCB2 activated PPARδ in ECs. (A) Model structures showing the complex formed by the PPARδ ligand-binding pocket and PCB2 based on molecular docking. PCB2 is shown in green. **(B)** Binding affinity of PCB2 to PPARδ. **(C)** BAECs were co-transfected with pPPRE-TK-luc with either pcDNA-PPARδ or pcDNA3.1 and treated with DMSO, PCB2 (10 μM) or GW501516 (1 μM) for 24 h. The luciferase activities were shown as fold changes in relation to the control (n = 4). **(D)** BAECs were transfected with pPPRE-TK-luc and PPARδ plasmids and then pretreated with or without GSK0660 (1 μM, 1 h) before the exposure to PCB2 (10 μM, 24 h) (n = 4). **(E)** HUVECs were pretreated with or without GSK0660 (1 μM, 1 h) before the exposure to PCB2 (10 μM) for 24 h. The mRNA levels of PDK4, ADRP and ANGPTL4 were assessed (n = 6). All data were expressed as mean ± SEM. *P < 0.05, **P < 0.01 vs. Vehicle; #P < 0.05, ##P < 0.01 vs. PCB2. (For interpretation of the references to colour in this figure legend, the reader is referred to the Web version of this article.)

3. Results

3.1. PCB2 attenuated high glucose-triggered ER stress in ECs

To investigate whether PCB2 attenuated ER stress in ECs, HUVECs were incubated with PCB2 (10 μM) or DMSO as the vehicle control for 12 h before the exposure to high glucose (HG, 30 mM) or tunicamycin (TM, 2 μg/ml) in the presence or absence of PCB2 for 24 h. As shown in Fig. 1A–D, the PERK arm of the UPR, including PERK phosphorylation, and protein levels of ATF4, GRP78 and PDI were increased in ECs after the treatments with HG or TM. PCB2 significantly attenuated the ER stress induced by HG or TM. In addition, we examined the other two arms of the UPR, i.e., IRE1α and ATF6 pathways. Our results showed that PCB2 also significantly mitigated the activation of IRE1α and ATF6 provoked by HG or TM (Fig. 1E–H). Furthermore, PCB2 also decreased the mRNA levels of the ER stress response genes including CHOP, GRP78, ATF4 and ATF3 induced by HG or TM (Fig. 1I–J).

Increased levels of circulating free fatty acids are among the most relevant risk factors in obesity, metabolic syndrome and type 2 diabetes.

groups. The vascular reactivity experiments were analyzed by using two-way ANOVA followed by Bonferroni post-tests. Values of P < 0.05 was considered statistically significant. All data was analyzed by using GraphPad Prism 8.0 (GraphPad Software, San Diego, CA, USA).

PA accounts for nearly 30% of saturated fatty acids in human and is known to stimulate ER stress and impair the endothelial dysfunction [3]. Thus, we examined the effects of PCB2 on the PA-induced ER stress in ECs. As shown in Figs. S1A–D, PCB2 also significantly inhibited the activation of PERK, IRE1α and ATF6 pathways induced by PA. Thus, we demonstrated that PCB2 effectively prevent ECs from aberrant UPR activated by high glucose and PA, two major metabolic insults in diabetes.

3.2. PCB2 activated PPARδ in ECs

We recently reported that nuclear receptor PPARδ alleviated ER stress and subsequent endothelial dysfunction in diabetic mice [21]. Thus, we hypothesized that PCB2 might mitigate ER stress via activation of PPARδ. Firstly, the AutoDock binding energy calculation indicated that PCB2 might favorably bind to PPARδ (binding energy -8.9 kcal/-mol) (Fig. 2A). We next performed SPR-based Biacore assay to detect the physical binding of PCB2 to PPARδ. As shown in Fig. 2B, PCB2 bound PPARδ with a relatively high affinity. Further, we performed luciferase reporter assay to functionally evaluate the ability of PCB2 to activate the PPARδ-driven gene transactivation. BAECs were transfected with pPPRE-TK-luc, together with pcDNA-PPARδ or pcDNA 3.1 as a negative control and then were exposed to PCB2 (10 μM) or a synthetic PPARδ ligand GW501516 (1 μM, as a positive control). As shown in Fig. 2C,
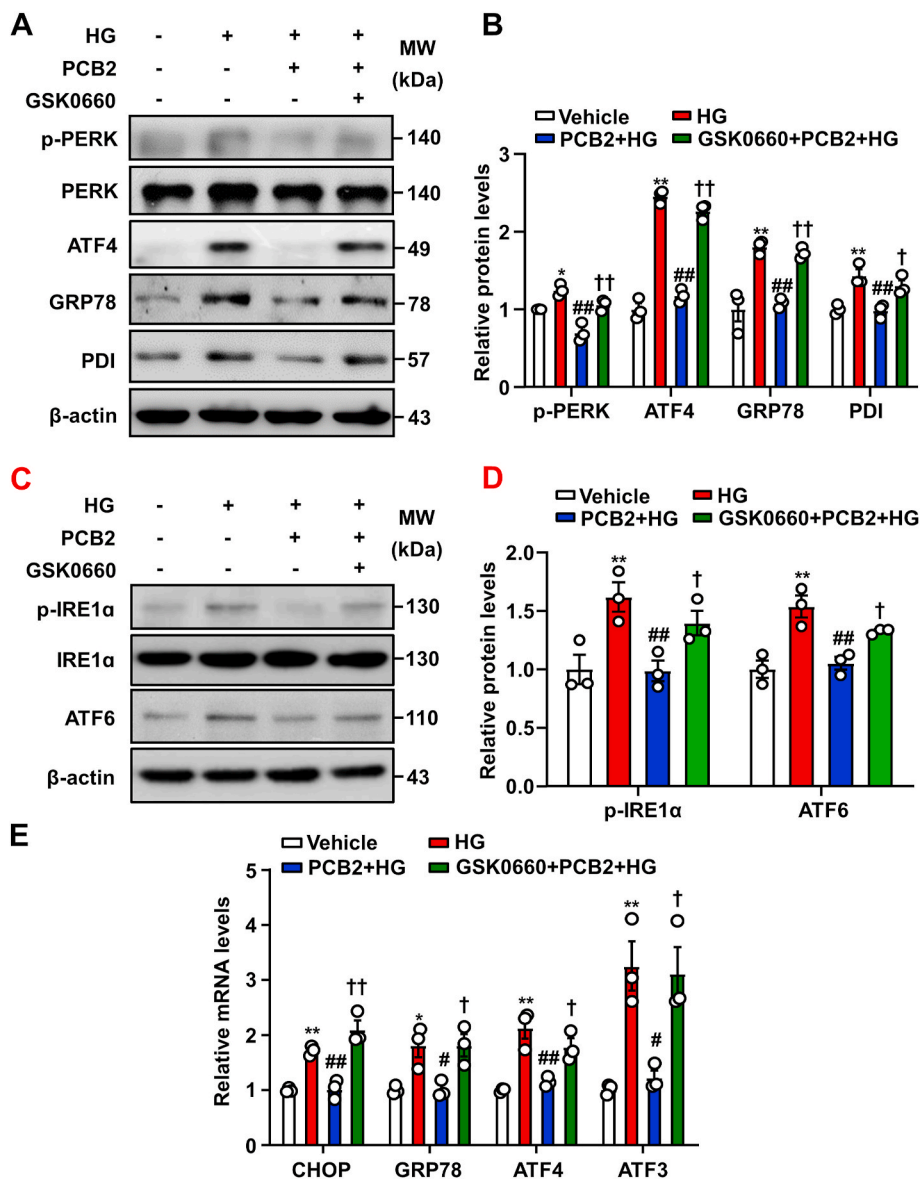
Fig. 3. Inhibition of PPARδ abrogated the suppressive effects of PCB2 on ER stress. **(A)** HUVECs were pretreated with or without GSK0660 (1 μM) for 1 h, then incubated with PCB2 (10 μM, 12 h) before the exposure to HG (30 mM, 24 h). Protein levels of p-PERK, PERK, ATF4, GRP78 and PDI were assessed. **(B)** Quantification of p-PERK/PERK, ATF4, GRP78 and PDI levels as in (A) (n = 3). **(C)** Protein levels of p-IRE1α, IRE1α and ATF6 were assessed. **(D)** Quantification of p-IRE1α/IRE1α and ATF6 levels as in (C) (n = 3). **(E)** The mRNA levels of CHOP, GRP78, ATF4 and ATF3 were assessed (n = 3). All data were expressed as mean ± SEM. *$P < 0.05$, **$P < 0.01$ vs. Vehicle; #$P < 0.05$, ##$P < 0.01$ vs. HG; †$P < 0.05$, ††$P < 0.01$ vs. PCB2+HG.

promoter reporter assays showed that PCB2 activated PPARδ-luciferase gene expression. Importantly, GSK0660, a selective PPARδ antagonist, abrogated the activation by PCB2 (Fig. 2D). Moreover, qRT-PCR showed that the gene expressions of endogenous PPARδ target genes ADRP, PDK4 and ANGPTL4 were increased by PCB2 and the inductions were antagonized by GSK0660 (Fig. 2E). Taken together, these results suggested that PCB2 might function as a phytochemical ligand to activate PPARδ in ECs.

3.3. PPARδ antagonist abrogated the PCB2 effects on ER stress

To determine whether PPARδ mediated the PCB2 effects on ER stress, HUVECs were pretreated with GSK0660 (1 μM, 1 h) and then with PCB2 (10 μM, 12 h) before the exposure to HG (30 mM) in the presence or absence of PCB2 for 24 h. As shown in Fig. 3A–E, in the presence of GSK0660, PCB2 failed to inhibit the activation of the PERK, IRE1α and ATF6 pathways induced by HG both at mRNA and protein levels. These results indicated that PCB2 attenuated HG-activated ER stress response via a PPARδ-dependent mechanism.

Next, we examined whether PCB2 could also mitigate the high glucose-induced ER stress in senescent ECs. To this end, we performed

the experiments using HUVECs after 12 consecutive passages. As shown in Figs. S2A–D, all three arms of the UPR pathways were activated by high glucose in these cells. PCB2 also effectively attenuated the excessive ER stress in the senescent ECs in a PPARδ-dependent manner.

3.4. PCB2 improved vascular relaxation impaired by high glucose

ER stress is implicated in endothelial dysfunction and leads to impaired vasorelaxation [22]. Therefore, we investigated the effects of PCB2 on ACh-induced EDR using mouse aortas. As shown in Fig. 4A–B, HG impaired vascular relaxation response to ACh. Notably, pre-treatment with PCB2 significantly improved the vasorelaxation. In contrast, SNP (a NO donor)-induced vasorelaxation was neither affected by HG nor modified by PCB2 pretreatment (Fig. 4C). It was indicated that PCB2 improved the high glucose-impaired vasorelaxation though an endothelium-dependent action.

Among the endothelium-derived factors regulating vascular relaxation, NO is produced by endothelial NO synthase (eNOS) from L-arginine and acts in a paracrine manner on soluble guanylyl cyclase (sGC) in vascular smooth muscle cells to cause vasorelaxation [23]. Thus, we further treated the artery rings with different pharmacological inhibitors
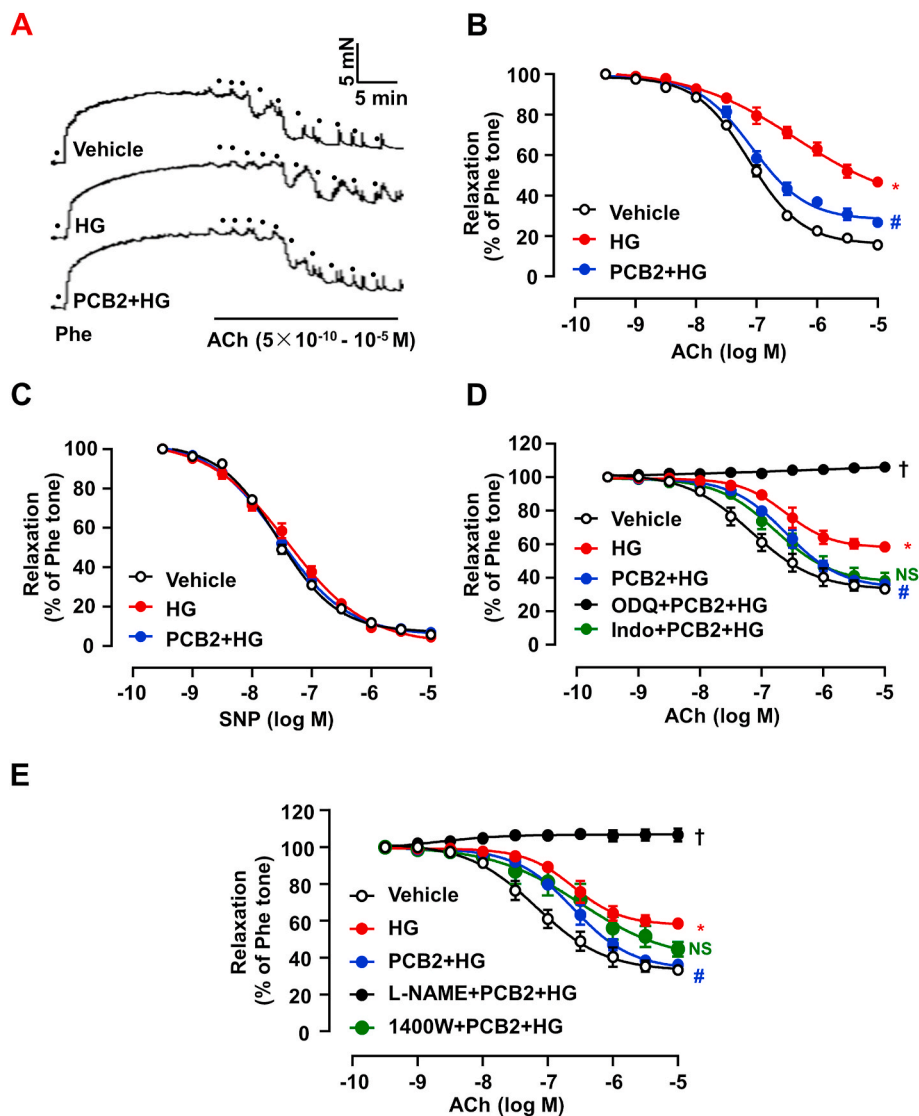
Fig. 4. PCB2 improved vascular relaxation impaired by high glucose. C57BL/6J mouse thoracic aortic rings were pretreated with PCB2 (10 μM, 12 h) or vehicle before the exposure to HG (30 mM, 36 h) or mannitol. **(A)** Representative traces of the ACh-induced relaxation of the Phe-precontracted rings. The dots represented cumulative addition of increasing doses of ACh (5×10^{-10} to 10^{-5} M). **(B)** PCB2 ameliorated the ACh-induced relaxations which were impaired by HG. **(C)** SNP-induced relaxations were not affected by HG. **(D)** Alternatively, the aortic rings were treated with indomethacin (Indo, 1 μM), ODQ (3 μM) or **(E)** L-NAME (100 μM) or 1400 W (100 nM) for 30 min before the Phe-contraction and ACh-induced relaxation. All data were expressed as mean ± SEM. n = 5, *$P < 0.05$ vs. Vehicle; #$P < 0.05$ vs. HG; ‡$P < 0.05$ vs. PCB2+HG; NS, not significant vs. PCB2+HG.

before the exposure to PCB2. As showed in Fig. 4D–E, either ODQ (an inhibitor of sGC) or L-NAME (an inhibitor of eNOS) abolished the protective effect of PCB2 on the HG-impaired vasorelaxation. However, neither indomethacin (Indo, an inhibitor of COX that synthesizes prostacyclin) nor 1400 W (an iNOS inhibitor) affected the PCB2 action. Taken together, these results demonstrated that the protective effect of PCB2 was dependent on eNOS-derived NO signaling.

3.5. PCB2 enhanced endothelium-dependent vasodilatation via PPARδ activation

To examine the role of PPARδ in the vasoprotective effect of PCB2, thoracic aortas from WT and PPARδ^EC-/- mice were treated with PCB2 and then exposed to high glucose. While PCB2 ameliorated high glucose-triggered endothelial dysfunction in WT littermate mice, such a protective effect was abrogated in the aortas from PPARδ^EC-/- mice (Fig. 5A–B). Similarly, the pharmacological antagonist of PPARδ, GSK0660, also abolished the PCB2 effect on EDR in the aortas from C57BL/6J mice (Fig. 5C).

In addition, PCB2 also ameliorated the PA-impaired relaxation in the aortas from WT mice but not the EC-specific PPARδ-deficient mice (Figs. S3A–B). Thus, these results suggested that PCB2 may activate PPARδ to mitigate endothelial dysfunction induced by multiple risk factors associated with diabetes.

3.6. Inhibition of PPARδ abrogated the effects of PCB2 on ROS and NO productions

ER stress and oxidative stress may co-exist and instigate each other to perturb cellular homeostasis [24]. In ECs, excessive ROS production triggers eNOS uncoupling and reduces NO bioavailability, leading to endothelial dysfunction [25]. Thus, we further examined the effects of PCB2 on ROS and NO levels. As shown in Fig. 6A–C, HG-stimulated ROS production was attenuated by PCB2. Importantly, the anti-oxidative capacity of PCB2 was largely attenuated in the presence of GSK0660. Measurement of intracellular NO using a fluorescence dye showed that HG-reduced NO production was prevented by PCB2. However, GSK0660 antagonized the effect of PCB2 on NO production (Fig. 6D). Since the level of nitrite, as a stable product of NO oxidization, indicated the production and release of unstable NO, we used the Griess reaction and determined the nitrite concentrations in the EC supernatants (Fig. 6E). These results suggested that PCB2 decreased ROS and increased NO production in ECs depending on PPARδ.
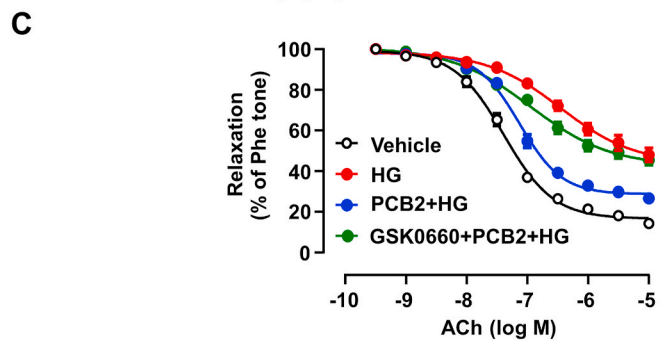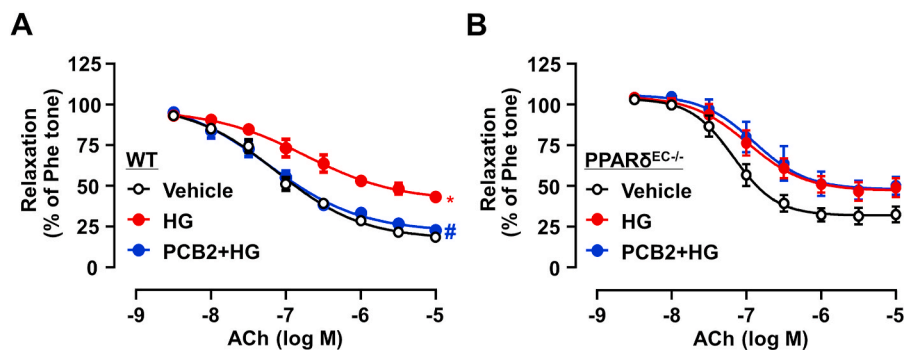
Fig. 5. PCB2 enhanced endothelium-dependent vasodilatation via PPARδ activation. Thoracic aortic rings were isolated from PPARδ WT littermates **(A)** or PPARδ[EC-/-] mice **(B)** and pretreated with PCB2 (10 μM, 12 h) before the exposure to HG (30 mM, 36 h). ACh-induced vasodilatory responses were measured (n = 5). **(C)** C57BL/6J mouse aortic rings were pretreated with GSK0660 (1 μM) for 1 h, then incubated with PCB2 (10 μM, 12 h) before the exposure to HG (30 mM, 36 h) (n = 5). All data were expressed as mean ± SEM. *$P < 0.05$ vs. Vehicle; #$P < 0.05$ vs. HG; †$P < 0.05$ vs. PCB2+HG.
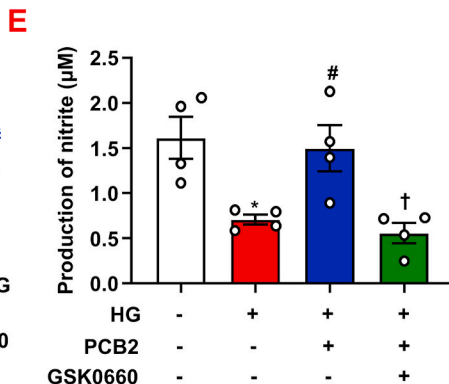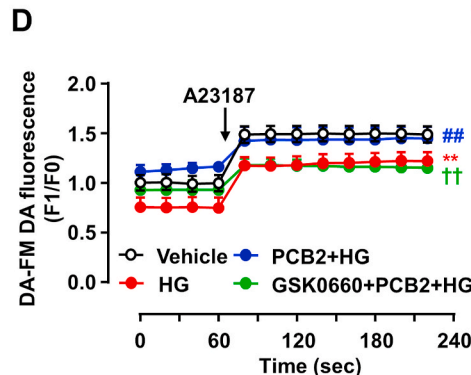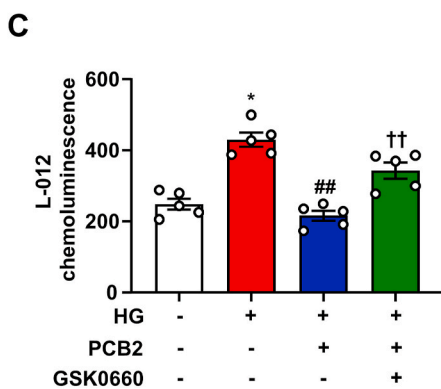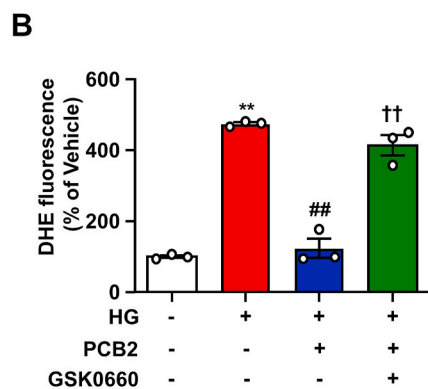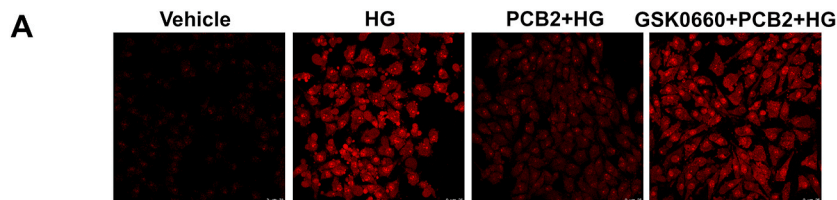
Fig. 6. Inhibition of PPARδ abrogated the effects of PCB2 on NO and ROS production. ECs were pretreated with GSK0660 (1 μM) for 1 h and then treated with PCB2 (10 μM) for 12 h before exposure to HG (30 mM) for 24 h. **(A)** Confocal microscopic detection of superoxide with DHE. **(B)** The mean fluorescence intensity was evaluated. Scale bar: 25 μm (n = 3). **(C)** Production of ROS was measured with L-012 chemiluminescence (n = 5). **(D)** Summerized levels of intracellular NO production in ECs detected as DAF FM-DA signals before (F0) and after (F1) the addition of A23187 (n = 5). **(E)** Nitrite levels in EC supernatants was measured by using the Griess reagent (n = 4). All data were expressed as mean ± SEM. *$P < 0.05$, **$P < 0.01$ vs. vehicle; #$P < 0.05$, ##$P < 0.01$ vs. HG; †$P < 0.05$, ††$P < 0.01$ vs. PCB2+HG.
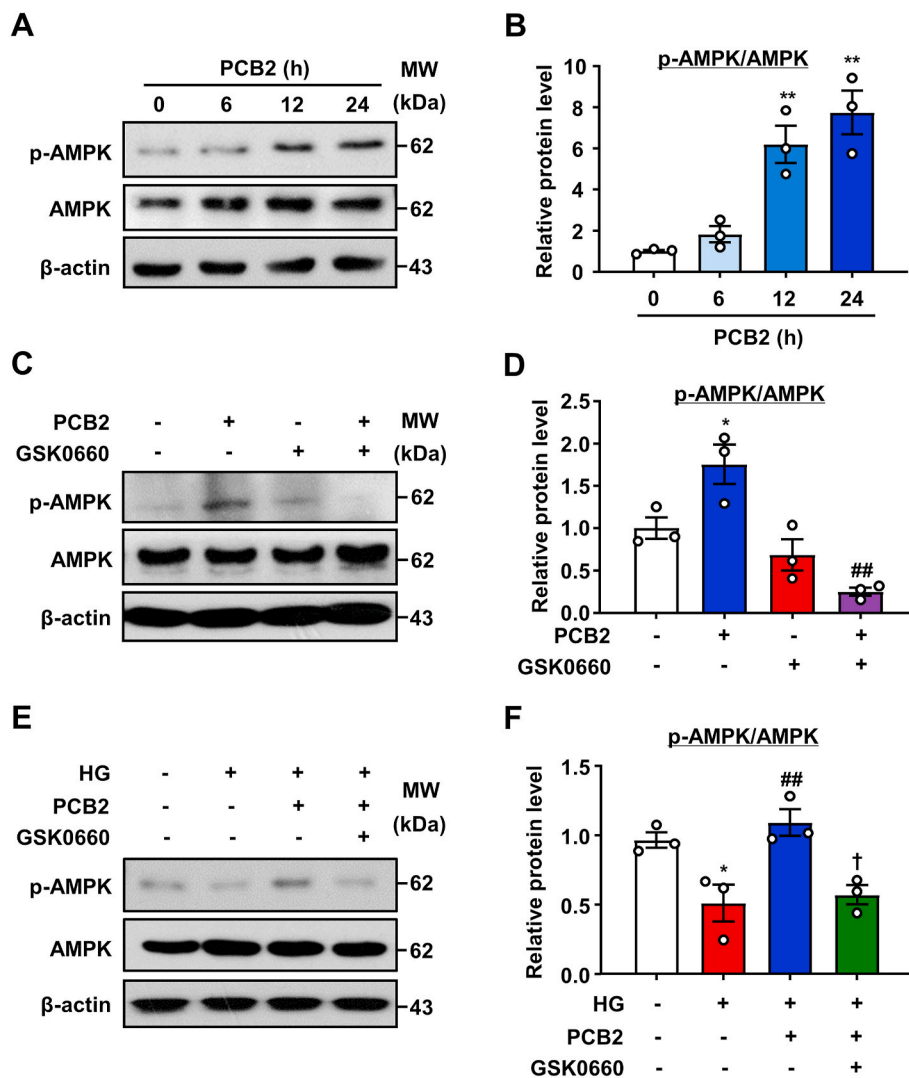
Fig. 7. PCB2 increased AMPK phosphorylation via PPARδ activation. (A) HUVECs were exposed to PCB2 (10 μM) for indicated time periods. Phosphorylated-AMPK and AMPK levels were detected. **(B)** Quantification of p-AMPK/AMPK level as in (A) (n = 3). All data were expressed as mean ± SEM. **$P < 0.01$ vs. vehicle. **(C)** HUVECs were treated with GSK0660 (1 μM) for 1 h before the exposure to PCB2 (10 μM) for 6 h, the levels of p-AMPK and AMPK were detected. **(D)** Quantification of p-AMPK/AMPK level as in (C) (n = 3). All data were expressed as mean ± SEM. *$P < 0.05$ vs. vehicle; ##$P < 0.01$ vs. PCB2. **(E)** HUVECs were pretreated with GSK0660 (1 μM, 1 h) and, then, incubated with PCB2 (10 μM, 12 h) before the exposure to HG (30 mM, 24 h). Protein levels of p-AMPK and AMPK were measured. **(F)** Quantification of p-AMPK/AMPK level as in (E) (n = 3). All data were expressed as mean ± SEM. *$P < 0.05$, **$P < 0.01$ vs. vehicle; ##$P < 0.01$ vs. HG; †$P < 0.05$ vs. PCB2+HG.

3.7. AMPK mediated the PCB2/PPARδ action in ECs

PPARδ and AMPK act synergistically to regulate metabolic programs [26]. We previously found that AMPK inhibited ER stress and the ensuing endothelial dysfunction [21]. Therefore, we examined the effect of PCB2 on AMPK phosphorylation in ECs. As shown in Fig. 7A–B, PCB2 increased the AMPK phosphorylation (Thr 172 on AMPKα). Notably, GSK0660 prevented the effects of PCB2 on AMPK phosphorylation under both basal and high-glucose conditions (Fig. 7C–F). These results indicated that PPARδ was required for PCB2 to activate AMPK.

In ECs, inhibition of AMPK with CC diminished the protective effects of PCB2 on ER stress (Fig. 8A–D). In mouse aortas, the effect of PCB2 on vasorelaxation was significantly attenuated when AMPK was inhibited by CC (Fig. 8E–F). These results indicated that the PPARδ-AMPK axis was required for the abilities of PCB2 in mitigating ER stress and endothelial dysfunction (Fig. 8G).

4. Discussion

In this study, we uncovered a novel mechanism by which PCB2 improves endothelial function. Our findings are as follows: 1) PCB2 ameliorated high glucose-triggered ER stress and endothelial dysfunction; 2) PCB2 activated PPARδ in ECs; 3) The suppressive effects of PCB2 on the ER stress were mediated via the activation of PPARδ.

Increased fruit and vegetable intake is associated with reduced risk of

major cardiovascular diseases, diabetes and all-cause mortality in Europe, US as well as Asia [27–29]. Recent studies have demonstrated additional beneficial effects of procyanidins on endothelial function. Procyanidins improved endothelium-dependent vasorelaxation, suppressed the synthesis of endothelin-1 (ET-1), a vasoconstrictive factor, and inhibited endothelial inflammation [30–32]. There is compelling evidence that reduction of ER stress would be a promising strategy to treat diabetes and other vascular diseases [33]. In the present study, we showed that PCB2 attenuated the activation of UPR pathways PERK, IRE1α and ATF6 in ECs (Fig. 1). Thus, mitigation of ER stress may represent an important mechanism by which procyanidins exert their cardiovascular protection.

Nuclear receptor PPARδ regulates many physiological processes such as cell growth and differentiation as well as wound healing [34]. PPARδ also has pivotal roles in endothelial homeostasis. Activation of PPARδ in ECs has a potent anti-inflammatory effect [19]. PPARδ improved the endothelial dysfunction in diabetic mice via the activation of PI3K/Akt/eNOS signaling pathways, suggesting the therapeutic potential of PPARδ agonists for diabetic vascular complications [35]. PPARδ was also required for the benefits of physical exercise and metformin on vascular health by reducing ER stress and oxidative stress [22]. Here, PPARδ activation appeared to be a major mechanism by which PCB2 suppressed the endothelial ER stress. This notion was supported by several lines of evidence: 1) molecular docking indicated that PCB2 fits into the ligand-binding pocket in PPARδ with a high affinity (Fig. 2A); 2)
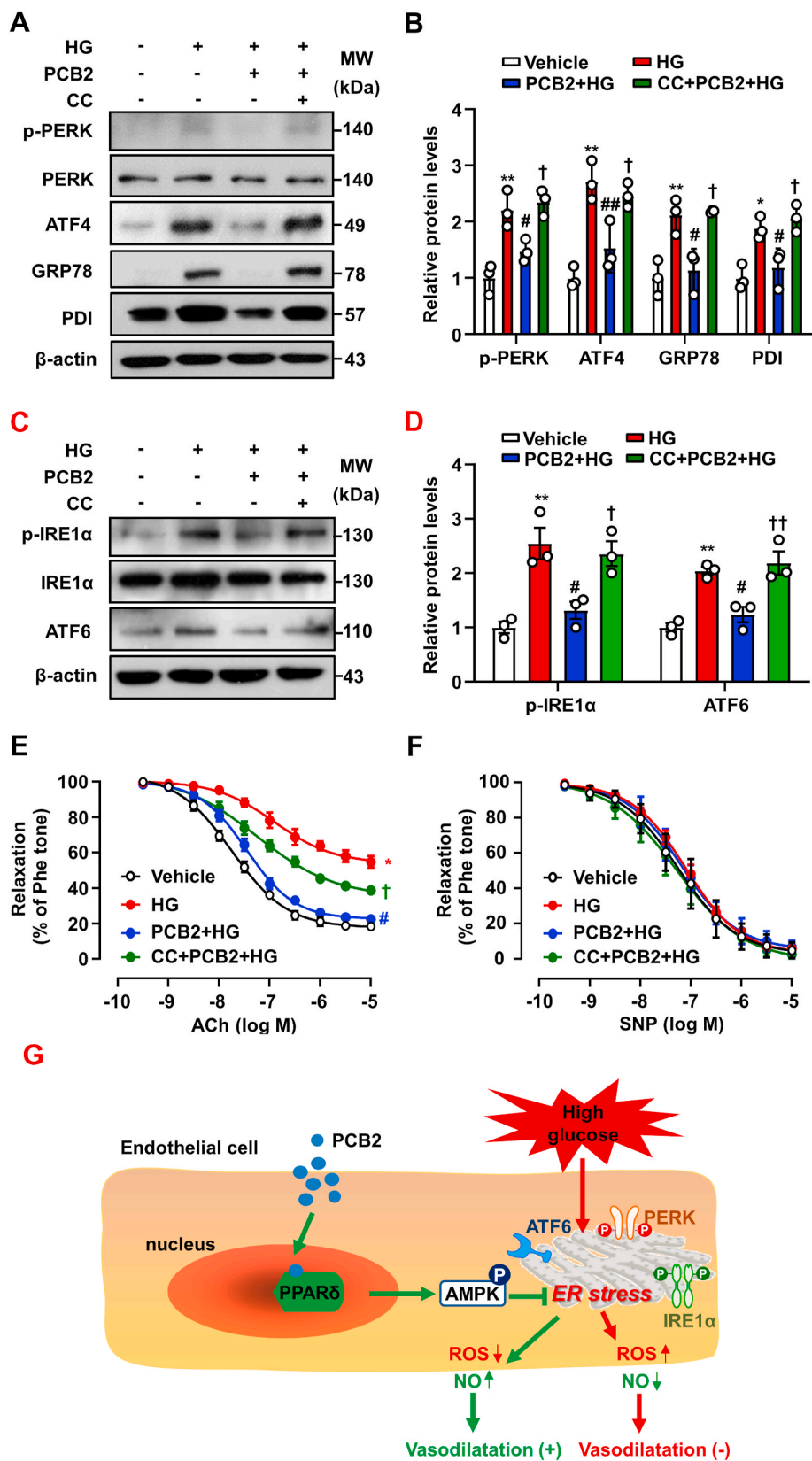
Fig. 8. AMPK activation mediated the PCB2/PPARδ improved endothelial function. (A) HUVECs were pretreated with compound C (CC, 20 μM, 1 h) and then incubated with PCB2 (10 μM, 12 h) before the exposure to HG (30 mM, 24 h). Protein levels of p-PERK, PERK, ATF4, GRP78 and PDI were measured. **(B)** Quantification of p-PERK/PERK, ATF4, GRP78 and PDI levels as in (A) (n = 3). **(C)** Protein levels of p-IRE1α, IRE1α and ATF6 were assessed. **(D)** Quantification of p-IRE1α/IRE1α and ATF6 levels as in (C) (n = 3). C57BL/6J mouse thoracic aortic rings were pretreated with CC (20 μM, 1 h) and, then, incubated with PCB2 (10 μM, 12 h) before the exposure to HG (30 mM, 36 h). **(E)** ACh-induced endothelium-dependent and **(F)** SNP-induced endothelium-independent relaxations were measured (n = 5). All data were expressed as mean ± SEM. *$P < 0.05$, **$P < 0.01$ vs. vehicle; #$P < 0.05$, ##$P < 0.01$ vs. HG; †$P < 0.05$, ††$P < 0.01$ vs. PCB2+HG. **(G)** The proposed mechanisms: PCB2 activated PPARδ-AMPK to prevent ER stress and ameliorated endothelial dysfunction against high glucose.

a physical interaction between PCB2 and PPARδ was detected by using the SPR assay (Fig. 2B); 3) a selective antagonist GSK0660 could block the activation of PPARδ by PCB2 in the luciferase reporter assay and the induction of the target genes (Fig. 2C–E); 4) PPARδ activity was indispensable for PCB2 to protect ECs against ER stress (Fig. 3). As expected, PCB2 significantly induced the expressions of the endogenous PPARδ target genes whereas the activity on the luciferase reporter was less robust compared to GW501516, which is a synthetic ligand

developed based on combinatorial chemistry and structure to acquire the full potency and selectivity [36].

A role of ER stress in endothelial dysfunction is highlighted by the results that suppression of ER stress with tauroursodeoxycholic acid (TUDCA) ameliorated endothelial dysfunction in the aortas and mesenteric arteries from diabetic db/db mice [37]. In fact, effects of TUDCA on endothelial function of T2DM patients are currently evaluated in a pilot clinical trial (NCT03462940). In our study, the PCB2-improved vasorelaxation was completely abolished by ʟ-NAME or ODQ, but not indomethacin, indicating that the vasorelaxation effect of PCB2 is dependent on NO-cGMP pathway (Fig. 4). ER stress could decrease eNOS expression and NO bioavailability via ROS generation in ECs [38] and was involved in endothelial dysfunction [39]. Therefore, it is likely that the effect of PCB2 on ROS production and NO bioavailability may account for its protection against the ER stress-triggered endothelial dysfunction.

AMPK is equally important player in the protective action of PCB2 against ER stress in ECs. As a serine/threonine kinase and the key sensor and modulator of cellular energy homeostasis, AMPK also regulates many other cellular processes including inflammation, autophagy and proliferation [40]. Here, we found that PCB2, as a natural ligand, activated PPARδ to mitigate endothelial ER stress. Yet, the inhibitor of AMPK also abrogated the PCB2 effects on the UPR pathways and HG-induced endothelial dysfunction. This could be explained by the previously recognized functional synergy between AMPK and PPARδ [26]. In terms of the ER stress and endothelial dysfunction, AMPK and PPARδ also appeared to be inter-dependent pathways [21,22]. Although the precise mechanism underlying the activation of AMPK by PCB2 remains to be explored, the roles of AMPK in the regulation of ER stress have been emerging. An early study using AMPKα-deficient mice established the critical role of AMPK in protecting ECs against ER stress by a mechanism involving sarco-endoplasmic reticulum calcium ATPase (SERCA) and intracellular Ca^{2+} homeostasis [41]. They also showed that the AMPK activation by metformin, statins or genetic manipulation inhibited endothelial ER stress in response to oxidized and glycated low-density lipoprotein via mitigating SERCA oxidization in high-fat fed ApoE/AMPKα2-deficent mice [8]. In addition, AMPK pathway also negate ER stress by inhibiting mTORC1 signaling to brake the protein synthesis and unfolding [42]. The inhibition of mTORC1 by AMPK could be achieved via the phosphorylation and activation of the mTOR suppressor TSC2 [43] or the phosphorylation and the ensuing inactivation of Raptor, a subunit of mTORC1 [44]. Moreover, AMPK might also mitigate ER stress by phosphorylating the downstream molecules such as CHOP [45].

Taken these interactive pathways into consideration, we proposed a putative mode for the actions of PCB2 (Fig. 8G). As a natural agonist, PCB2 binds to and activates the PPARδ, which interacts with AMPK to mitigate the high glucose-provoked UPR pathways (PERK, IRE1α and ATF6) and regulates ROS production and NO bioavailability, leading to improved endothelial function.

Declaration of competing interest

The authors declare that they have no conflict of interest.

Acknowledgements

Appendix A. Supplementary data

Supplementary data to this article can be found online at https://doi.org/10.1016/j.redox.2020.101728.

Author contributions

L.X: designed the study, analyzed the results, and revised the manuscript. N.W: designed the study, analyzed the results, and revised the manuscript. X.N: performed most of experiments, analyzed the data, and drafted the manuscript. W.T: performed most of experiments, analyzed the data, and drafted the manuscript. Z.Z: participated in the study. C.Y: participated in the study. L.Q: participated in the study. E.Q: participated in the study. X.X: participated in the study. J.Z: participated in the study. W.Z: participated in the study.

References

[1] P. Walter, D. Ron, The unfolded protein response: from stress pathway to homeostatic regulation, Science 334 (2011) 1081–1086.

[2] C. Hetz, The unfolded protein response: controlling cell fate decisions under ER stress and beyond, Nat. Rev. Mol. Cell Biol. 13 (2012) 89–102.

[3] M.L. Battson, D.M. Lee, C.L. Gentile, Endoplasmic reticulum stress and the development of endothelial dysfunction, Am. J. Physiol. Heart Circ. Physiol. 312 (2017) H355–H367.

[4] G.S. Hotamisligil, Endoplasmic reticulum stress and the inflammatory basis of metabolic disease, Cell 140 (2010) 900–917.

[5] M. Civelek, E. Manduchi, R.J. Riley, C.J. Stoeckert, P.F. Davies, Chronic endoplasmic reticulum stress activates unfolded protein response in arterial endothelium in regions of susceptibility to atherosclerosis, Circ. Res. 105 (2009), 453-U127.

[6] C.W. Younce, K.K. Wang, P.E. Kolattukudy, Hyperglycaemia-induced cardiomyocyte death is mediated via MCP-1 production and induction of a novel zinc-finger protein MCPIP, Cardiovasc. Res. 87 (2010) 665–674.

[7] N.M. Borradaile, X.L. Han, J.D. Harp, S.E. Gale, D.S. Ory, J.E. Schaffer, Disruption of endoplasmic reticulum structure and integrity in lipotoxic cell death, J. Lipid Res. 47 (2006) 2726–2737.

[8] Y.Z. Dong, M.A. Zhang, S.X. Wang, B. Liang, Z.X. Zhao, C. Liu, M.Y. Wu, H.C. Choi, T.J. Lyons, M.H. Zou, Activation of AMP-activated protein kinase inhibits oxidized LDL-triggered endoplasmic reticulum stress in vivo, Diabetes 59 (2010) 1386–1396.

[9] S. Lenna, R. Han, M. Trojanowska, Endoplasmic reticulum stress and endothelial dysfunction, IUBMB Life 66 (2014) 530–537.

[10] H.C. Hung, K.J. Joshipura, R. Jiang, F.B. Hu, D. Hunter, S.A. Smith-Warner, G. A. Colditz, B. Rosner, D. Spiegelman, W.C. Willett, Fruit and vegetable intake and risk of major chronic disease, J. Natl. Cancer Inst. 96 (2004) 1577–1584.

[11] H. Zhang, R. Tsao, Dietary polyphenols, oxidative stress and antioxidant and anti-inflammatory effects, Curr Opin Food Sci 8 (2016) 33–42.

[12] N. Martinez-Micaelo, N. Gonzalez-Abuin, M. Pinent, A. Ardevol, M. Blay, Procyanidin B2 inhibits inflammasome-mediated IL-1 beta production in lipopolysaccharide-stimulated macrophages, Mol. Nutr. Food Res. 59 (2015) 262–269.

[13] H. Alkhalidy, Y. Wang, D. Liu, Dietary flavonoids in the prevention of T2D: an overview, Nutrients 10 (2018).

[14] R.R. Holt, S.A. Lazarus, M.C. Sullards, Q.Y. Zhu, D.D. Schramm, J.F. Hammerstone, C.G. Fraga, H.H. Schmitz, C.L. Keen, Procyanidin dimer B2 [epicatechin-(4 beta-8)-epicatechin] in human plasma after the consumption of a flavanol-rich cocoa, Am. J. Clin. Nutr. 76 (2002) 798–804.

[15] Y. Xiao, Z.Z. Hu, Z.T. Yin, Y.M. Zhou, T.Y. Liu, X.L. Zhou, D.W. Chang, Profiling and distribution of metabolites of procyanidin B2 in mice by UPLC-DAD-ESI-IT-TOF-MSn technique, Front. Pharmacol. 8 (2017).

[16] Z. Zhang, X. Xie, Q. Yao, J. Liu, Y. Tian, C. Yang, L. Xiao, N. Wang, PPARdelta agonist prevents endothelial dysfunction via induction of dihydrofolate reductase gene and activation of tetrahydrobiopterin salvage pathway, Br. J. Pharmacol. 176 (2019) 2945–2961.

[17] G. Cima, AVMA guidelines for the Euthanasia of animal: 2013 edition, Javma-J Am Vet Med A. 242 (2013) 715–716.

[18] D.G. Drescher, N.A. Ramakrishnan, M.J. Drescher, Surface plasmon resonance (SPR) analysis of binding interactions of proteins in inner-ear sensory epithelia, Methods Mol. Biol. 493 (2009) 323–343.

[19] Y. Fan, Y. Wang, Z. Tang, H. Zhang, X. Qin, Y. Zhu, Y. Guan, X. Wang, B. Staels, S. Chien, N. Wang, Suppression of pro-inflammatory adhesion molecules by PPAR-delta in human vascular endothelial cells, Arterioscler. Thromb. Vasc. Biol. 28 (2008) 315–321.

[20] X. Xie, Z. Zhang, X. Wang, Z. Luo, B. Lai, L. Xiao, N. Wang, Stachydrine protects eNOS uncoupling and ameliorates endothelial dysfunction induced by homocysteine, Mol. Med. 24 (2018) 10.

[21] W.S. Cheang, X.Y. Tian, W.T. Wong, C.W. Lau, S.S.T. Lee, Z.Y. Chen, X.Q. Yao, N. P. Wang, Y. Huang, Metformin protects endothelial function in diet-induced obese mice by inhibition of endoplasmic reticulum stress through 5' adenosine monophosphate-activated protein kinase-peroxisome proliferator-activated receptor delta pathway, Arterioscler. Thromb. Vasc. Biol. 34 (2014) 830–836.

[22] W.S. Cheang, W.T. Wong, L. Zhao, J. Xu, L. Wang, C.W. Lau, Z.Y. Chen, R.C. Ma, A. Xu, N. Wang, X.Y. Tian, Y. Huang, PPARdelta is required for exercise to attenuate endoplasmic reticulum stress and endothelial dysfunction in diabetic mice, Diabetes 66 (2017) 519–528.

[23] Y.Z. Zhao, P.M. Vanhoutte, S.W.S. Leung, Vascular nitric oxide: beyond eNOS, J. Pharmacol. Sci. 129 (2015) 83–94.

[24] S.S. Cao, R.J. Kaufman, Endoplasmic reticulum stress and oxidative stress in cell fate decision and human disease, Antioxidants Redox Signal. 21 (2014) 396–413.

[25] Y.M. Yang, A. Huang, G. Kaley, D. Sun, eNOS uncoupling and endothelial dysfunction in aged vessels, Am. J. Physiol. Heart Circ. Physiol. 297 (2009) H1829–H1836.

[26] V.A. Narkar, M. Downes, R.T. Yu, E. Embler, Y.X. Wang, E. Banayo, M.M. Mihaylova, M.C. Nelson, Y. Zou, H. Juguilon, H. Kang, R.J. Shaw, R.M. Evans, AMPK and PPARdelta agonists are exercise mimetics, Cell 134 (2008) 405–415.

[27] F.L. Crowe, A.W. Roddam, T.J. Key, P.N. Appleby, K. Overvad, M.U. Jakobsen, A. Tjonneland, L. Hansen, H. Boeing, C. Weikert, J. Linseisen, R. Kaaks, A. Trichopoulou, G. Misirli, P. Lagiou, C. Sacerdote, V. Pala, D. Palli, R. Tumino, S. Panico, H.B. Bueno-de-Mesquita, J. Boer, C.H. van Gils, J.W.J. Beulens, A. Barricarte, L. Rodriguez, N. Larranaga, M.J. Sanchez, M.J. Tormo, G. Buckland, E. Lund, B. Hedblad, O. Melander, J.H. Jansson, P. Wennberg, N.J. Wareham, N. Slimani, I. Romieu, M. Jenab, J. Danesh, V. Gallo, T. Norat, E. Riboli, E.P.I.C. N, Fruit and vegetable intake and mortality from ischaemic heart disease: results from the European Prospective Investigation into Cancer and Nutrition (EPIC)-heart study, Eur. Heart J. 32 (2011) 1235–1243.

[28] H.D. Du, L.M. Li, D. Bennett, Y. Guo, T.J. Key, Z. Bian, P. Sherliker, H.Y. Gao, Y.P. Chen, L. Yang, J.S. Chen, S.Q. Wang, R.R. Du, H. Su, R. Collins, R. Peto, Z.M. Chen, C.K.B. Study, Fresh fruit consumption and major cardiovascular disease in China, N. Engl. J. Med. 374 (2016) 1332–1343.

[29] V. Miller, A. Mente, M. Dehghan, S. Rangarajan, X.H. Zhang, S. Swaminathan, G. Dagenais, R. Gupta, V. Mohan, S. Lear, S.I. Bangdiwala, A.E. Schutte, E. Wentzel-Viljoen, A. Avezum, Y. Altuntas, K. Yusoff, N. Ismail, N. Peer, J. Chifamba, R. Diaz, O. Rahman, N. Mohammadifard, F. Lana, K. Zatonska, A. Wielgosz, A. Yusufali, R. Iqbal, P. Lopez-Jaramillo, R. Khatib, A. Rosengren, V.R. Kutty, W. Li, J.K. Liu, X.Y. Liu, L. Yin, K. Teo, S. Anand, S. Yusuf, P.S. Investigators, Fruit, vegetable, and legume intake, and cardiovascular disease and deaths in 18 countries (PURE): a prospective cohort study, Lancet 390 (2017) 2037–2049.

[30] A. Novakovic, M. Marinko, G. Jankovic, I. Stojanovic, P. Milojevic, D. Nenezic, V. Kanjuh, Q. Yang, G.W. He, Endothelium-dependent vasorelaxant effect of procyanidin B2 on human internal mammary artery, Eur. J. Pharmacol. 807 (2017) 75–81.

[31] R. Corder, W. Mullen, N.Q. Khan, S.C. Marks, E.G. Wood, M.J. Carrier, A. Crozier, Red wine procyanidins and vascular health, Nature 444 (2006), 566-566.

[32] H.X. Yang, L. Xiao, Y. Yuan, X.Q. Luo, M.L. Jiang, J.H. Ni, N.P. Wang, Procyanidin B2 inhibits NLRP3 inflammasome activation in human vascular endothelial cells, Biochem. Pharmacol. 92 (2014) 599–606.

[33] T. Minamino, I. Komuro, M. Kitakaze, Endoplasmic reticulum stress as a therapeutic target in cardiovascular disease, Circ. Res. 107 (2010) 1071–1082.

[34] N.P. Wang, PPAR-delta in vascular pathophysiology, PPAR Res. 2008 (2008).

[35] W.T. Wong, X.Y. Tian, Y. Huang, PPARdelta activation protects endothelial function in diabetic mice via PI3K/Akt/eNOS signaling pathway, Circulation 124 (2011).

[36] W.R. Oliver Jr., J.L. Shenk, M.R. Snaith, C.S. Russell, K.D. Plunket, N.L. Bodkin, M.C. Lewis, D.A. Winegar, M.L. Sznaidman, M.H. Lambert, H.E. Xu, D.D. Sternbach, S.A. Kliewer, B.C. Hansen, T.M. Willson, A selective peroxisome proliferator-activated receptor delta agonist promotes reverse cholesterol transport, Proc. Natl. Acad. Sci. U. S. A. 98 (2001) 5306–5311.

[37] Y. Dong, C. Fernandes, Y. Liu, Y. Wu, H. Wu, M.L. Brophy, L. Deng, K. Song, A. Wen, S. Wong, D. Yan, R. Towner, H. Chen, Role of endoplasmic reticulum stress signalling in diabetic endothelial dysfunction and atherosclerosis, Diabetes Vasc. Dis. Res. 14 (2017) 14–23.

[38] M. Galan, M. Kassan, P.J. Kadowitz, S. Belmadani, K. Matrougui, Mechanism of endoplasmic reticulum stress-induced vascular endothelial dysfunction, Biochim. Biophys. Acta 1843 (2014) 1063–1075.

[39] M. Kassan, M. Galan, M. Partyka, Z. Saifudeen, D. Henrion, M. Trebak, K. Matrougui, Endoplasmic reticulum stress is involved in cardiac damage and vascular endothelial dysfunction in hypertensive mice, Arterioscler. Thromb. Vasc. Biol. 32 (2012) 1652–1661.

[40] D. Garcia, R.J. Shaw, AMPK: mechanisms of cellular energy sensing and restoration of metabolic balance, Mol. Cell. 66 (2017) 789–800.

[41] Y.Z. Dong, M. Zhang, B. Liang, Z.L. Xie, Z.X. Zhao, S. Asfa, H.C. Choi, M.H. Zou, Reduction of AMP-activated protein kinase alpha 2 increases endoplasmic reticulum stress and atherosclerosis in vivo, Circulation 121 (2010) 792–803.

[42] H. Li, Q. Min, C. Ouyang, J. Lee, C. He, M.H. Zou, Z. Xie, AMPK activation prevents excess nutrient-induced hepatic lipid accumulation by inhibiting mTORC1 signaling and endoplasmic reticulum stress response, Biochim. Biophys. Acta 1842 (2014) 1844–1854.

[43] K. Inoki, T.Q. Zhu, K.L. Guan, TSC2 mediates cellular energy response to control cell growth and survival, Cell 115 (2003) 577–590.

[44] D.M. Gwinn, D.B. Shackelford, D.F. Egan, M.M. Mihaylova, A. Mery, D.S. Vasquez, B.E. Turk, R.J. Shaw, AMPK phosphorylation of raptor mediates a metabolic checkpoint, Mol. Cell. 30 (2008) 214–226.

[45] X.Y. Dai, Y. Ding, Z.Y. Liu, W.C. Zhang, M.H. Zou, Phosphorylation of CHOP (C/EBP homologous protein) by the AMP-activated protein kinase alpha 1 in macrophages promotes CHOP degradation and reduces injury-induced neointimal disruption in vivo, Circ. Res. 119 (2016) 1089–1100.